International Journal of Agricultural Sciences
Volume 20 | Issue 1 | January, 2024 | 226-235 ■ ISSN : 0973-130X
DOI:10.15740/HAS/IJAS/20.1/226-235
Visit us : *www.researchjournal.co.in*

***RESEARCH PAPER***

# Time series analysis and development of simulation model for monthly rainfall using ARIMA model

P. A. Damor[1], A. A. Mod[2], Bhavin Ram* **and** H. V. Parmar[1]
Department of Soil and Water Engineering, College of Agricultural Engineering and Technology, Junagadh Agricultural University, Junagadh (Gujarat) India (Email : bhavinram@aau.in)

**Abstract :** Rainfall holds critical significance for water resource applications, particularly in rainfed agricultural systems. This study employs the Autoregre ssive Integrated Moving Average (ARIMA) technique, a data mining approach commonly used for time series analysis and future forecasting. Given the increasing importance of climate change forecasting in averting unexpected natural hazards such as floods, frost, forest fires, and droughts, accurate weather data forecasting becomes imperative. The objective of this study was to develop a Seasonal Auto-Regressive Integrative Moving Average (SARIMA) model for forecasting monthly rainfall in Junagadh Station, Gujarat. Utilizing 50 years of historical data (1968 to 2016), the SARIMA model predicts weekly rainfall for the subsequent five years (2018 to 2022). Through comprehensive evaluation using ACF and PACF plots, AIC, SBC, MAPE, and MAE values, the study identifies SARIMA $(1,0,0)(3,1,1)_{12}$ as the optimal model, offering the most accurate prediction. The robust results affirm that the SARIMA model provides reliable and satisfactory weekly rainfall predictions. This research contributes valuable insights into the precision and efficacy of SARIMA models for rainfall forecasting, aiding in strategic water resource management in the Junagadh region.

**Key Words :** SARIMA, AIC, BIC, MAPE, SIC

**View Point Article :** Damor, P. A., Mod, A. A., Ram, Bhavin and Parmar, H. V. (2023). Time series analysis and development of simulation model for monthly rainfall using ARIMA model. *Internat. J. agric. Sci.*, **20** (1) : 226-235, **DOI:10.15740/HAS/IJAS/20.1/226-235.**


**Article History : Received :** 19.09.2023; **Revised :** 25.10.2023; **Accepted :** 27.11.2023

## INTRODUCTION

Efficient water resource management relies heavily on accurately forecasting rainfall for a given area or station (Kumar *et al.*, 2021; Kumar *et al.*, 2021a and Kumar *et al.,* 2022). Rainfall, a critical hydrological parameter, plays a crucial role in tasks such as irrigation planning, runoff modeling, and drought and flood management. The dynamic nature of rainfall patterns, influenced by changing climatic conditions, poses challenges such as flooding, landslides, and drought (Shivhare *et al.*, 2017), significantly impacting agriculture and farming. In the context of Indian agriculture, the southwest monsoon (June-September) holds a pivotal role in the agrarian economy, with adequate rainfall being essential for robust crop production (Kumar *et al.*, 2021). The nonlinear and complicated nature of rainfall makes accurate prediction challenging. The accuracy and

***Author for correspondence:**
[1]Junagadh Agricultural University, Junagadh (Gujarat) India (Email:padamor@jau.in)
[2]Gujarat Vidyapeeth (Anand Agricultural University), Ahmedabad (Gujarat) India

adequacy of rainfall data serve as the cornerstone for determining the ultimate success of any progressive endeavors in natural resource management. Runoff characteristics, in terms of both quantity and quality, in the majority of watersheds across micro to macro scales, are significantly shaped and controlled by spatiotemporal variations in rainfall (Ram, Bhavin *et al.*, 2023a). Due to the adverse effects of climate change, rainfall patterns are rapidly changing, and short-term and long-term forecasts of rainfall hold significant relevance for agriculture, tourism, flood prevention and management strategies, and water body management, all of which influence a country's economy. Accurately predicting future climate data is a challenging task (Nikam and Meshram, 2013). Various techniques, including numerical and machine learning processes based on historical time series and radar data, have been adopted for rainfall prediction (Chander *et al.*, 2002; Ingsrisawang *et al.*, 2008). Currently, the most common methodology for rainfall prediction involves using radar image data from various organizations and analyzing them. However, various statistical methods are often useful for predicting rainfall (Bisgaard and Kulahci, 2011).

Among these methods, one of the most effective approaches for analyzing time series data is the model introduced by Box and Jenkins (1976) and modified by Box et al. (1994), also known as ARIMA (Autoregressive Integrated Moving Average). ARIMA has been widely employed over the years to predict rainfall trends (Mahsin *et al.,* 2012; Kaushik and Singh, 2008; Shamsnia *et al*., 2011; Thapaliyal, 1981; Momani *et al*., 2009), as well as for reservoir and river modeling (Dizon, 2007; Cui, 2011; Peng *et al.*, 2000 and Valipour *et al.*, 2012), economics and production (Nochai *et al.*, 2006) and evapotranspiration (Valipour, 2012). Forecasting involves predicting future values using this ordered data. Stochastic models evolving over time (Box and Jenkins, 1994) encompass autoregressive (AR) models, moving average (MA) models of different orders (Gupta and Kumar, 1994, and Verma, 2004) and autoregressive moving average (ARMA) models of discrete orders (Katz and Skaggs, 1981; Chhajed, 2004 and Katimon and Demon, 2004) for annual streamflow.

To address the forecasting challenge, two widely used algorithms, ARIMA and SARIMA, come into play. ARIMA considers past values (autoregressive, moving average) to predict future values, while SARIMA incorporates seasonality patterns, making it more potent for forecasting complex data spaces containing cycles. The ARIMA model emerges as a valuable tool, handling various dimensions related to univariate time series model selection, parameter optimization, and prediction. In the current study, our focus was on developing a seasonal rainfall forecasting model to predict the monthly rainfall time series for Junagadh city in Gujarat, India, utilizing 55 years (1965-2022) of monthly rainfall data.

## MATERIAL AND METHODS

**Study location :**

Junagadh is located between latitude 21°31'23.29" N and longitude 70°27'17.90" E, situated at an altitude of 86 meters above mean sea level in the South Saurashtra region of Gujarat state. The climate in this area is characterized as subtropical and semi-arid, with an average annual rainfall of 929.81 mm, primarily concentrated between mid-June and mid-October. The average annual pan evaporation is 5.6 mm/day. In terms of temperature, January is the coldest month, with a mean monthly temperature ranging from 7°C to 15°C. The peak of maximum monthly temperatures occurs in May, ranging between 29.50°C to 39.40°C. Relative humidity in the region fluctuates between 45% and 89%, and wind speeds vary from 2 to 9.70 km/h.

**Data :**

This study utilized monthly rainfall data covering a period of 55 years (1965-2022), sourced from the Agrometeorology Department of Junagadh Agricultural University, Junagadh. Predictive modeling was conducted for the five-year span (2018-2022) employing a seasonal ARIMA model, leveraging historical data from the preceding 50 years.

**Methodological description :**

*Auto Regressive Integrated Moving Average (ARIMA) model* :

In general, an ARIMA model is characterized by the notation ARIMA (p, d, q) where, p, d, and q denote orders of auto-regression, integration (differencing) and moving average, respectively. In ARIMA parlance, time series is a linear function of past actual values and random shocks. For instance, given a time series process $y_t$, a first order auto-regressive process is denoted by ARIMA (1, 0, 0) or simply AR (1) and is given by

$$y_t = \mu + \phi_1 y_{t-1} + \varepsilon_t$$

and a first order moving average process is denoted by ARIMA (0,0,1) or simply MA(1) and is given by

$$y_t = \mu - \theta_1 \varepsilon_{t-1} + \varepsilon_t$$

Alternatively, the model ultimately derived, may be mixture of these processes and of higher orders as well. Thus a stationary ARMA (p, q) process is defined by the equation :

$$y_t = \phi_1 y_{t-1} + \phi_2 y_{t-2} + \cdots + \phi_p y_{t-p} - \theta_1 \varepsilon_{t-1} - \theta_2 \varepsilon_{t-2} - \cdots - \theta_q \varepsilon_{t-q} + \varepsilon_t$$

Where $\varepsilon_t$ are independently and normally distributed with zero mean and constant variance $\sigma^2$ for t = 1, 2,…. n.

## Seasonal ARIMA modelling :

Identification of relevant models and inclusion of suitable seasonal variables are necessary for seasonal. The Seasonal ARIMA *i.e.* ARIMA (p, d, q) (P, D, Q)$_s$ model is defined by :

$$\phi_p(B)\varnothing_P(B^s)\nabla^d \nabla_s^D y_t = \Theta_Q(B^s)\theta_q(B)\varepsilon_t$$

where,

$\phi_p(B) = 1 - \phi_1 B - \cdots \phi_p B^p$ = Non-seasonal autoregressive (AR) operator

$\theta_q(B) = 1 - \theta_1 B - \cdots - \theta_q B^q$ =Non -seasonal moving average operator (MA) operator

$\varnothing_P(B^s) = 1 - \varnothing_1 B^s - \cdots - \varnothing_p B^{sP}$ = Seasonal auto regressive (SAR) operator

$\Theta_Q(B^s) = 1 - \Theta_1 B^s - \cdots - \Theta_Q B^{sQ}$ = Seasonal moving average operator (SMA)

Here,

B is the backshift operator (*i.e.* $B^1 y_t = y_{t-1}$, $B^2 y_t = y_{t-2}$ and so on) s is the seasonal lag and $\varepsilon_t$ is sequence of independent normal error variables with mean zero and variance '$\sigma^2$'.

p and q are orders of non-seasonal auto-regression and moving average parameters respectively and P and Q are that of the seasonal auto regression and moving average parameter respectively.

d and D denote the non-seasonal and seasonal differences, respectively.

## Art of ARIMA Model building :

*Identification* :

The first step in the process of modelling is to check for the stationarity of the series, as the estimation procedure are available only for stationary series. There are two kinds of stationarity, *viz.,* stationarity in 'mean' and stationarity in 'variance'. The chief tool in identification is auto-correlation function, partial autocorrelation function and the resulting correlogram. A cursory look at the graph of the data and structure of autocorrelation and partial correlation coefficients may provide clues for the presence of stationarity. Another way of checking for stationarity is to fit first order autoregressive model for the raw data and test whether the co-efficient 'ϕ1' is less than one. If the model is found to be non-stationary, stationarity could be achieved mostly by differencing the series.

Thus if '$y_t$' denotes the original series, the non-seasonal difference of first order is :

$$y_t' = y_t - y_{t-1}$$

and the seasonal difference of the first order is :

$$y_t' = y_t - y_{t-s}$$

where,

S is the length of season.

The next step in the identification process is to find the initial values for the orders of seasonal and non-seasonal parameters, p, q, and P, Q. They could be obtained by looking for significant autocorrelation and partial autocorrelation co-efficients.

*Estimation* :

At the identification stage one or more models are tentatively chosen that seem to provide statistically adequate representations of the available data. Then we attempt to obtained precise estimates of parameters of the model by least squares as advocated by Box and Jenkins. Standard computer packages like SAS, SPSS etc. are available for finding the estimates of relevant parameters using iterative procedures.

## Diagnostics :

Different models can be obtained for various combinations of AR and MA individually and collectively. The best model is obtained with the following diagnostics.

– Low Akaike Information Criteria (AIC)
Bayesian Information Criteria (BIC)
Schwarz-Bayesian Criteria (SBC)
– Plot of residual ACF
– MAPE
– MAE

## Evaluation criteria :

The other statistical criteria adopted in the study are:

**Akaike Information Criterion (AIC) :**

The AIC is given by

$$AIC = n\ln\sigma^2 + n + \frac{2(k+1)}{n-k-2} \quad (1)$$

Where $n$ is the size of the sample used for fitting, $k$ is the number of parameters excluding constant terms, and $\sigma^2(\varepsilon)$ is the maximum likelihood estimate of the residual variance.

**Schwarz information criterion (SIC) :**

The SIC is given by

$$SIC = n\ln\sigma^2(\varepsilon) + n + k\ln n \quad (2)$$

Where $n$, $k$ and are defined in the same way as for the AIC statistic.

**Mean absolute percentage error (MAPE):**

$$MAPE = \frac{1}{N}\sum_{i=1}^{N}\left|\frac{X_t - O_t}{O_t}\right| \times 100 \quad (3)$$

Where $X_t$= forecast value at time t; $O_t$= actual value at time t; N= number of weeks considered for forecasting.

**Mean absolute error (MAE) :**

$$MAE = \frac{1}{N}\sum_{i=1}^{N}|X_t - O_t| \quad (4)$$

Where $X_t$= forecast value at time t; $O_t$= actual value at time t; N= number of weeks considered for forecasting.

## Results and Discussion

In the present study the time series of monthly rainfall data from 1968 to 2017 (50 years) were used to develop the Seasonal ARIMA (SARIMA) model and the prediction was made for next five years (2018-2022) using the developed model. The forecasted values than used for validation of developed SARIMA model.

**Analysis of monthly rainfall time series used for model development :**

Data of monthly rainfalls were analysed using Statistical Analysis System (SAS) software. Auto correlation function (ACF) and Partial Auto correlation function (PACF) of the original time series of monthly rainfall are shown in Fig. 1.

A comprehensive analysis of the monthly rainfall time series data, covering the years 1968 to 2017, was undertaken, yielding key statistical insights. The mean monthly rainfall was computed at 78.39, accompanied by a substantial standard deviation of 156.56, indicating noteworthy variability in the dataset. With a total of 600 observations (N), the Augmented Dickey-Fuller (ADF) test results were noteworthy, revealing significant negative values for the Zero Mean ADF (-14.29), Single Mean ADF (-16.70), and Trend ADF (-16.69).

These ADF test statistics strongly suggest a high likelihood of non-stationarity in the time series data. Consistently low p-values associated with the ADF tests indicate a rejection of the Null hypothesis of non-stationarity. The negative values further underscore the presence of a stable trend in the data, establishing a solid foundation for the application of time series forecasting models. Table 1 presents diagnostic measures for the time series, featuring autocorrelation (AutoCorr) and partial correlation (Partial) co-efficients at different lags. The Ljung-Box Q statistic, along with associated p-values, is employed to test the Null hypothesis of no autocorrelation in the residuals. Notably, all autocorrelation co-efficients at various lags are deemed significant, evident from the low p-values (<0.0001). The

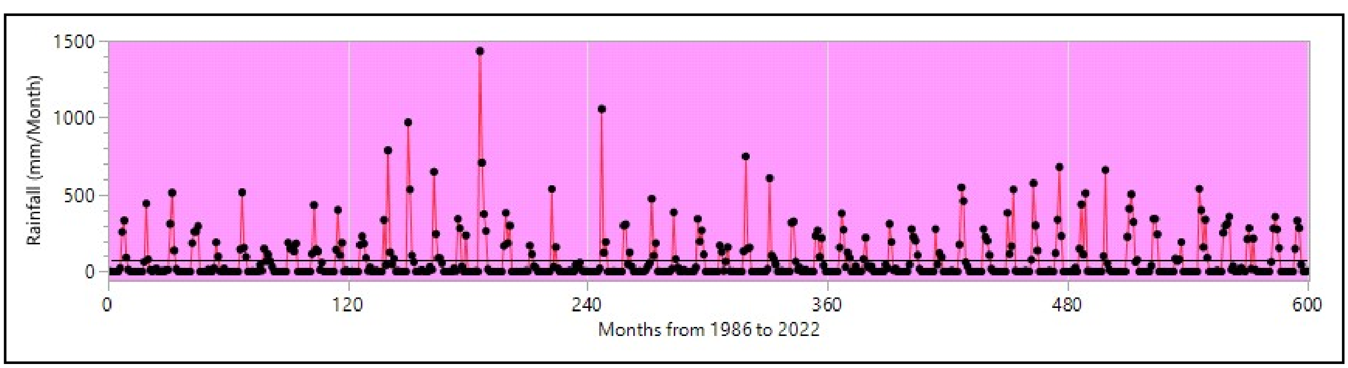


**Fig. 1 : Graph of monthly rainfall data series from 1968 to 2012**

**Table 1: Autocorrelation (Auto Corr) and partial correlation (Partial) co-efficients at different lags**

| Lag | Auto Corr | Ljung-Box Q | p-Value | Lag | Partial |
|---|---|---|---|---|---|
| 0 | 1 | | | 0 | 1 |
| 1 | 0.362773234 | 79.35812375 | 5.181E-19 | 1 | 0.36277323 |
| 2 | 0.104241467 | 85.92150433 | 2.2E-19 | 2 | -0.0315098 |
| 3 | -0.08575626 | 90.3709415 | 1.823E-19 | 3 | -0.1306381 |
| 4 | -0.21458977 | 118.2783508 | 1.245E-24 | 4 | -0.1609795 |
| 5 | -0.23929058 | 153.0385272 | 3.01E-31 | 5 | -0.1165981 |
| 6 | -0.24279555 | 188.8846944 | 4.392E-38 | 6 | -0.1370198 |
| 7 | -0.21103434 | 216.0115402 | 4.632E-43 | 7 | -0.1313705 |
| 8 | -0.20151928 | 240.7891393 | 1.541E-47 | 8 | -0.1784623 |
| 9 | -0.10637934 | 247.7054558 | 3.043E-48 | 9 | -0.0976508 |
| 10 | 0.125032667 | 257.2761342 | 1.6E-49 | 10 | 0.10175041 |
| 11 | 0.292593218 | 309.7763342 | 7.618E-60 | 11 | 0.14314757 |
| 12 | 0.445781499 | 431.8478948 | 6.728E-85 | 12 | 0.25989312 |
| 13 | 0.355190448 | 509.4783615 | 1.42E-100 | 13 | 0.12967677 |
| 14 | 0.082195966 | 513.642749 | 1.19E-100 | 14 | -0.0717863 |
| 15 | -0.08876629 | 518.5078064 | 6.85E-101 | 15 | -0.0422185 |
| 16 | -0.19790737 | 542.7325302 | 3.1E-105 | 16 | -0.0383614 |
| 17 | -0.23059581 | 575.6769615 | 2E-111 | 17 | -0.0320043 |
| 18 | -0.23662321 | 610.425732 | 5.38E-118 | 18 | -0.0446573 |
| 19 | -0.22543324 | 642.0199419 | 6.72E-124 | 19 | -0.0586822 |
| 20 | -0.20193839 | 667.4154872 | 1.72E-128 | 20 | -0.0890756 |
| 21 | -0.09270129 | 672.776425 | 7.44E-129 | 21 | -0.0356056 |
| 22 | 0.074300497 | 676.2262999 | 8E-129 | 22 | -0.027988 |
| 23 | 0.386031829 | 769.512662 | 9.62E-148 | 23 | 0.22149892 |
| 24 | 0.378157771 | 859.1876478 | 6.36E-166 | 24 | 0.02726229 |
| 25 | 0.362085604 | 941.5450073 | 1.44E-182 | 25 | 0.13170636 |

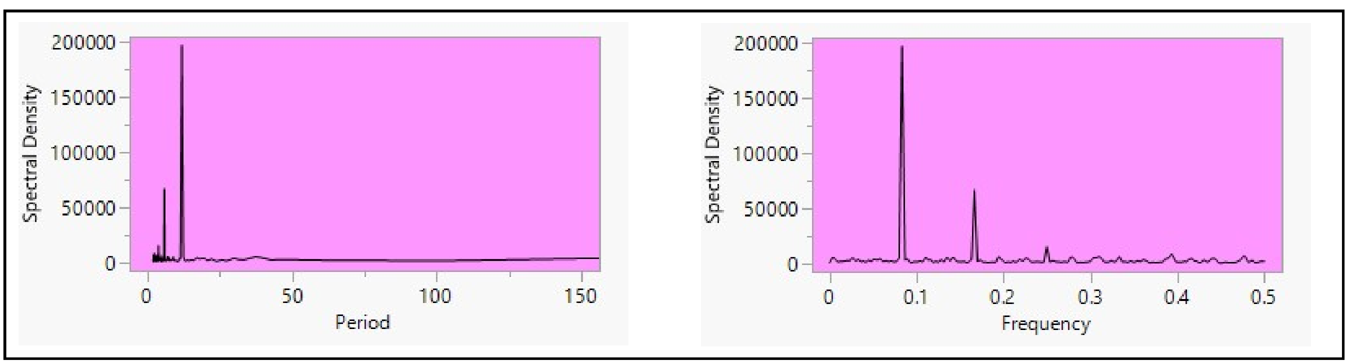


**Fig.2: Spectral density plots of monthly rainfall time series**

decreasing pattern in autocorrelation co-efficients with increasing lags indicates a diminishing influence of past observations on the current one. Moreover, the negative partial correlation co-efficients suggest that the model adequately captures the effect of past observations. These findings affirm the suitability of the model for forecasting, aligning with the assumption of white noise residuals—a crucial element for robust time series modeling. This robust analysis provides a solid basis for confident predictions and insights into the underlying patterns of the monthly rainfall time series.

**Model development and parameter estimation :**

Fig. 3 and 4 intricately illustrate the Autocorrelation Function (ACF) and Partial Autocorrelation Function (PACF), offering deep insights into the periodic nature of variables associated with monthly rainfall. These visual representations consistently unveil patterns suggestive of seasonal variations within the time series. Based on these observations, we posit a yearly period of 12 months for the monthly rainfall time series.

Transitioning to Fig. 5 and 6, they succinctly present an overview of the SARIMA (1,0,0) (3,1,1)12 model's performance in predicting monthly rainfall. Fig. 5 visually portrays the model's predictions, highlighting its proficiency in capturing both non-seasonal and seasonal components. The parameters (1,0,0) denote the presence of non-seasonal autoregressive effects and the absence of non-seasonal moving average effects. Meanwhile, (3,1,1) signifies first-order differencing, third-order autoregression, and first-order moving average in the seasonal part for achieving stationarity. This visualization provides a clear understanding of how well the SARIMA model aligns with observed monthly rainfall trends.

Moving to Fig. 6, the Residual Plot for SARIMA (1,0,0) (3,1,1)12 facilitates a rapid assessment of model residuals. A well-behaved residual plot indicates a well-fitted model. Analyzing this plot offers insights into the accuracy and reliability of the SARIMA model in predicting monthly rainfall, enhancing our confidence in the model's forecasting capabilities.

Fig. 3 and 4 intricately illustrate the Autocorrelation Function (ACF) and Partial Autocorrelation Function (PACF), offering deep insights into the periodic nature of variables associated with monthly rainfall. These visual representations consistently unveil patterns suggestive

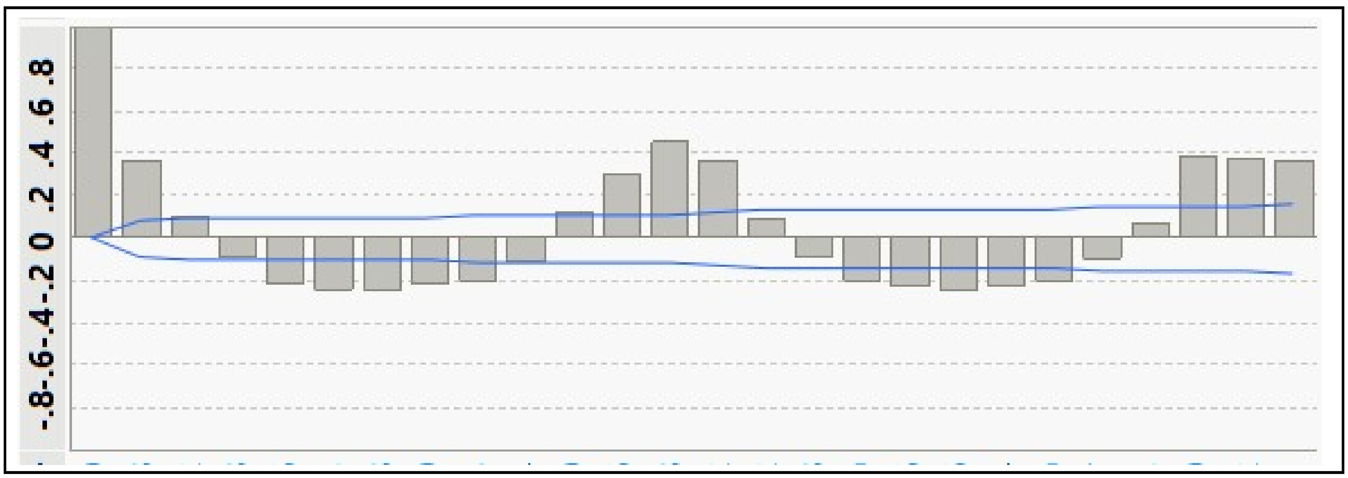


**Fig. 3: ACF plot of monthly rainfall time series**

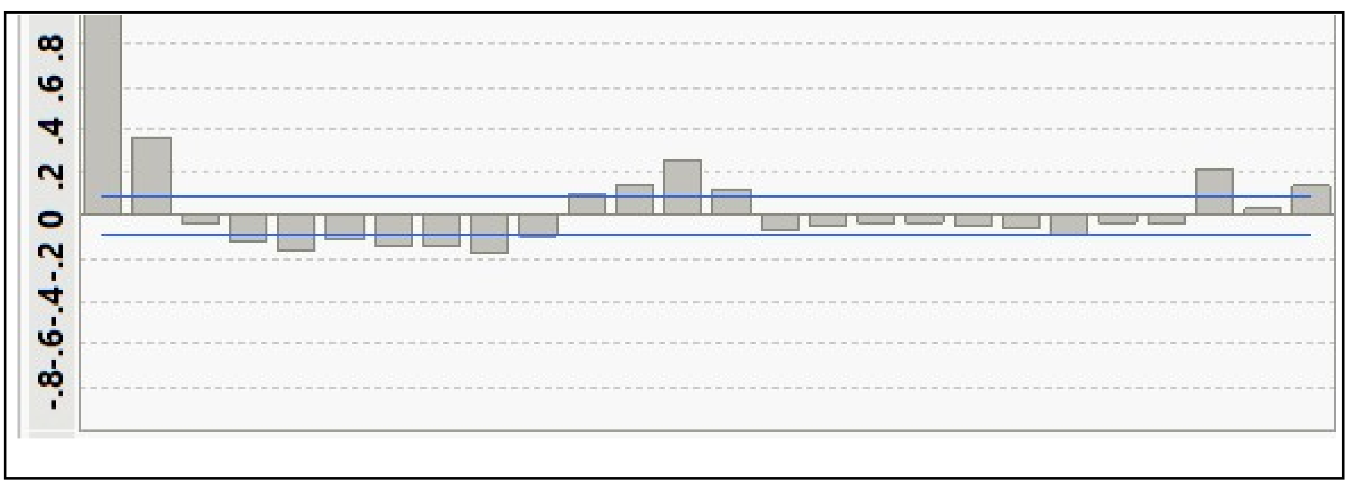


**Fig. 4 : PACF plot of monthly rainfall time series**

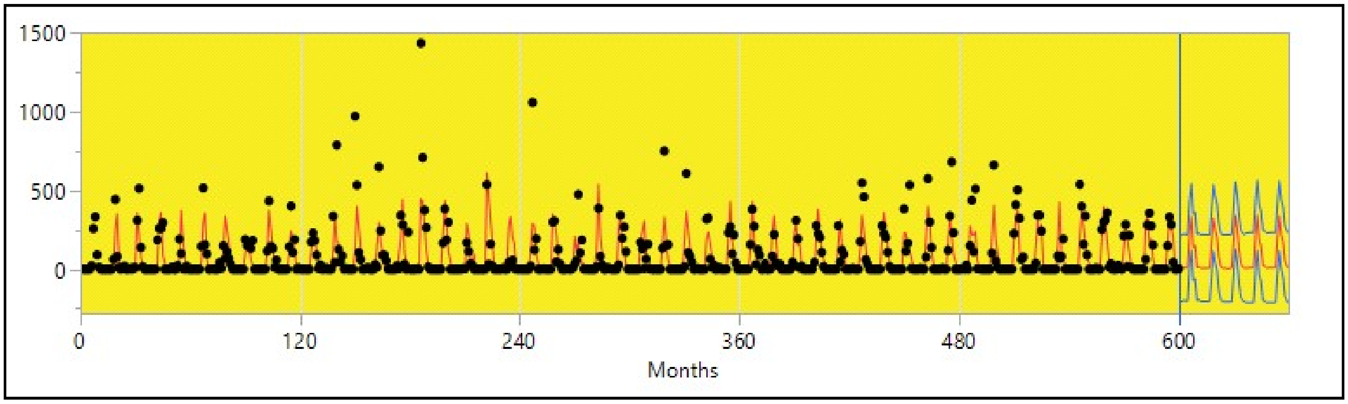


**Fig. 5 : Prediction of monthly rainfall using SARIMA SARIMA (1,0,0) $(3,1,1)_{12}$**

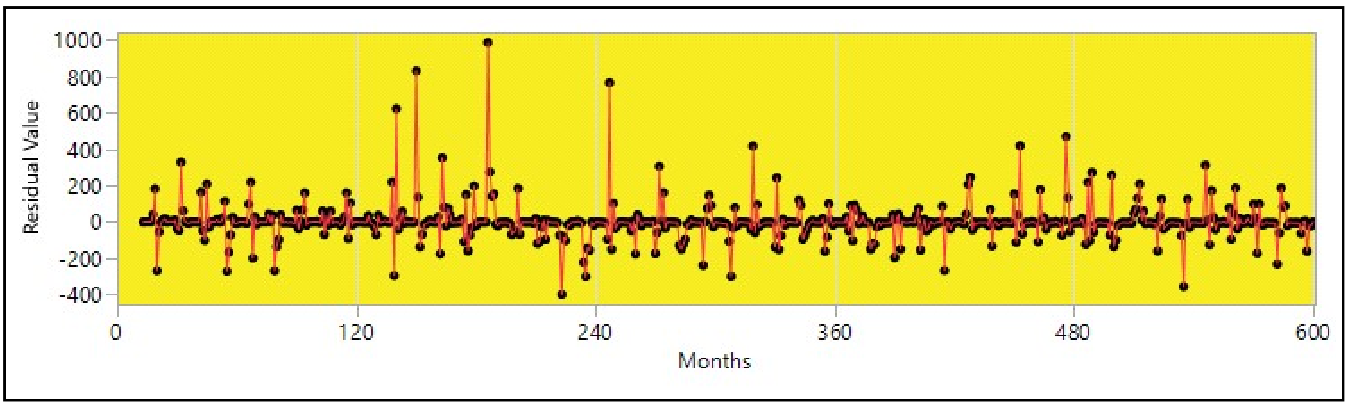


**Fig. 6 : Residual plot for SARIMA SARIMA (1,0,0) $(3,1,1)_{12}$**

of seasonal variations within the time series. Based on these observations, we posit a yearly period of 12 months for the monthly rainfall time series. Transitioning to Fig. 5 and 6, they succinctly present an overview of the SARIMA (1,0,0) (3,1,1)12 model's performance in predicting monthly rainfall. Fig. 5 visually portrays the model's predictions, highlighting its proficiency in capturing both non-seasonal and seasonal components. The parameters (1,0,0) denote the presence of non-seasonal autoregressive effects and the absence of non-seasonal moving average effects. Meanwhile, (3,1,1) signifies first-order differencing, third-order

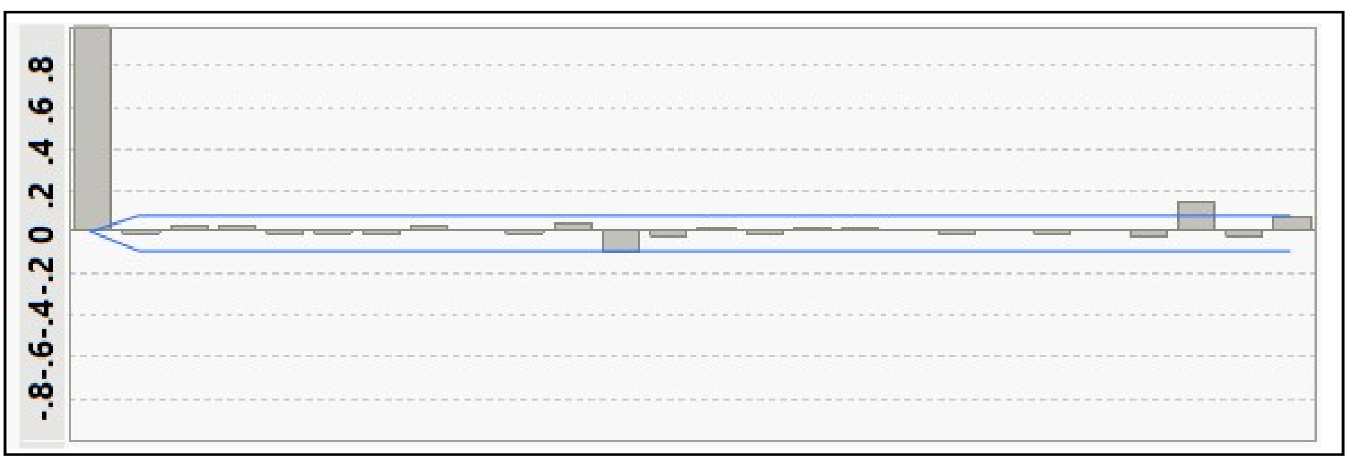


**Fig. 7: ACF plot for SARIMA (1,0,0) $(3,1,1)_{12}$**

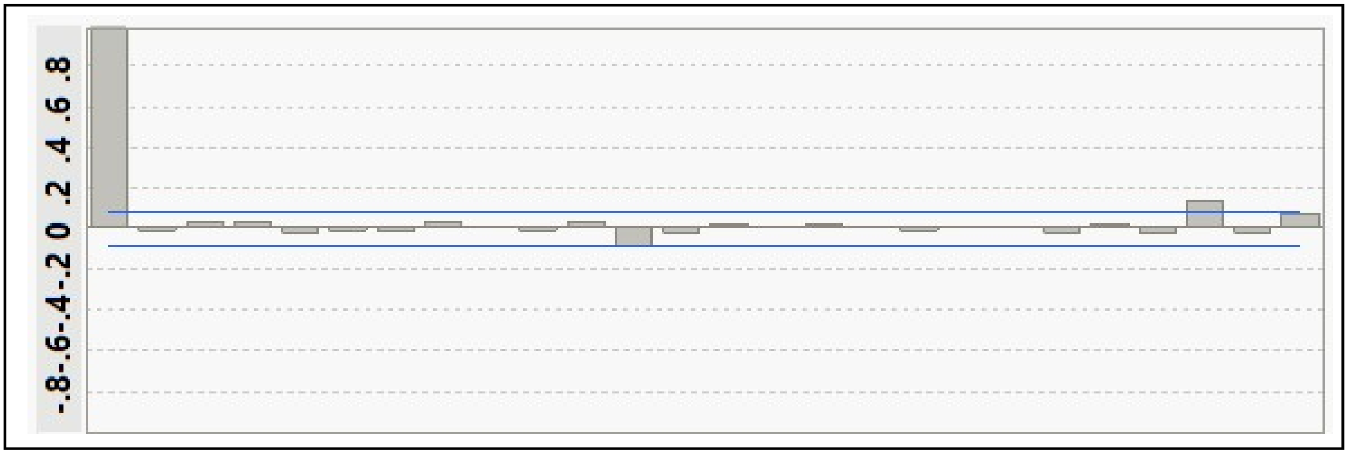


**Fig. 8 : PACF plot for SARIMA (1,0,0) $(3,1,1)_{12}$**

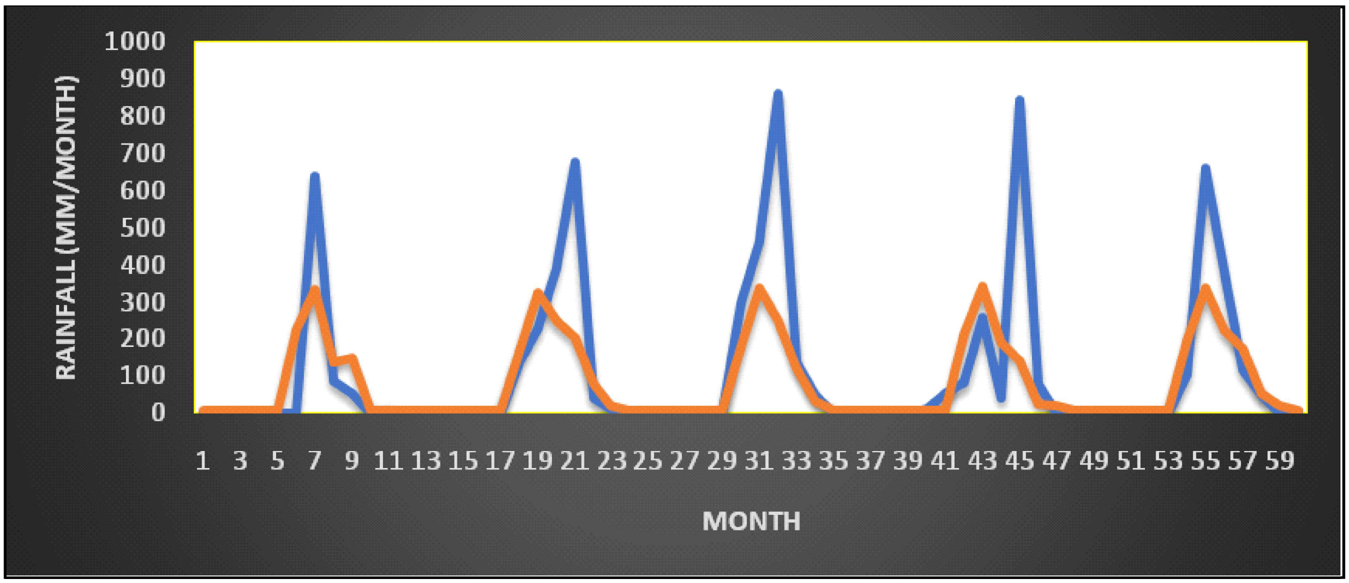


**Fig. 9: Comparison of actual and predicted monthly rainfall value of five years (2018-2022)**

**Table 2 : SARIMA (1,0,0) $(3,1,1)_{12}$ Model summary**

| DF | 582 |
|---|---|
| Sum of Squared Innovations | 6637600.919 |
| Sum of Squared Residuals | 7123072.847 |
| Variance Estimate | 11404.81258 |
| Standard Deviation | 106.7933171 |
| Akaike's 'A' Information Criterion | 7215.142629 |
| Schwarz's Bayesian Criterion | 7241.402991 |
| R Square | 0.510830092 |
| R Square Adj | 0.506627601 |
| MAPE | |
| MAE | 51.42976052 |
| -2LogLikelihood | 7203.142629 |

autoregression, and first-order moving average in the seasonal part for achieving stationarity. This visualization provides a clear understanding of how well the SARIMA model aligns with observed monthly rainfall trends. Moving to Fig. 6, the Residual Plot for SARIMA (1,0,0) (3,1,1)12 facilitates a rapid assessment of model residuals. A well-behaved residual plot indicates a well-fitted model. Analyzing this plot offers insights into the accuracy and reliability of the SARIMA model in predicting monthly rainfall, enhancing our confidence in the model's forecasting capabilities.

**Comparison of actual and predicted monthly rainfall value:**

Fig. 9 acts as a visual benchmark for comparing

**Table 3: SARIMA (1,0,0) $(3,1,1)_{12}$ parameter estimates**

| Term | Factor | Lag | Estimate | Std Error | t Ratio | Prob>\|t\| |
|---|---|---|---|---|---|---|
| AR1,1 | 1 | 1 | 0.101395 | 0.042153 | 2.405389 | 0.016466 |
| AR2,12 | 2 | 12 | 0.010925 | 0.04172 | 0.261858 | 0.793524 |
| AR2,24 | 2 | 24 | -0.16084 | 0.040183 | -4.00278 | 7.07E-05 |
| AR2,36 | 2 | 36 | 0.294941 | 0.040286 | 7.3211 | 8.22E-13 |
| MA2,12 | 2 | 12 | 1 | 0.025375 | 39.40842 | 2.1E-166 |
| Intercept | 1 | 0 | 0.273369 | 0.381115 | 0.717287 | 0.473485 |

actual and predicted values of monthly rainfall throughout the five-year period from 2018 to 2022. The graph meticulously scrutinizes the efficacy of the SARIMA model in forecasting monthly rainfall, revealing a striking alignment between the predicted time series and the actual data series. A close examination underscores the noteworthy proximity, showcasing the SARIMA model's exceptional ability to offer precise and reliable forecasts of rainfall patterns. The visual coherence observed in Fig. 9 is indicative of the model's adeptness in capturing the subtle nuances and fluctuations inherent in the observed data. This underscores the SARIMA model's effectiveness as a valuable forecasting tool. The visual representation not only provides a comprehensive endorsement but also serves as a compelling testament to the robust performance of the SARIMA model in predicting monthly rainfall values. This visual evidence reinforces our confidence in the model's accuracy and reinforces its practical utility in anticipating future rainfall trends.

## Conclusion :

In this study, a thorough examination of 50 years of monthly rainfall data (1968-2017) led to the development and validation of a Seasonal Autoregressive Integrated Moving Average (SARIMA) model. The model successfully predicted monthly rainfall for the subsequent five years (2018-2022). Key statistical insights revealed a mean monthly rainfall of 78.39 with a notable standard deviation of 156.56, emphasizing dataset variability.The Augmented Dickey-Fuller (ADF) test indicated non-stationarity in the time series data, supported by consistently low p-values and negative ADF test values, confirming a stable trend. Autocorrelation and partial correlation analyses demonstrated significant values with diminishing influences of past observations.Spectral density plots, ACF, and PACF plots guided the identification of seasonal variations, leading to the selection of a 12-month period for the SARIMA (1,0,0) (3,1,1) model. The model adeptly captured both non-seasonal and seasonal components, as validated by Figures 5 and 6 and further supported by a well-behaved Residual Plot.

The SARIMA model, anchored in extensive monthly rainfall data, proves to be a robust forecasting tool. Its precision and reliability make it invaluable for anticipating future rainfall trends, providing essential insights for effective water resource management and planning in the Junagadh region. The study highlights the SARIMA model's efficacy within the Box-Jenkins methodology, empowering decision-makers with strategic foresight to navigate the dynamic nature of climatic conditions and fortify water resources against uncertainties.

## REFERENCES

**Bender, M. and Stohodan, S. (1994) .**Time-series modelling for long-range stream flow forecasting. *Journal of Water Resources Planning & Management, ASCE,* **120**(6): 857-870.

**Box, G.E.P. and Jenkins, G.M. (1994).** Time series analysis, forecasting and control, Revised Edition, Holden-Day, San Francisco, California, United States.

**Chander, R.E. and Wheater, H.S. (2002).** Analysis of rainfall variability using generalized linear models: A case study from the west of Ireland. *Water Resour. Res.,* **38**(10) : 10-11

**Gupta, R.K. and Kumar, R. (1994).** Stochastic analysis of weekly evaporation values, *Indian J. Agric. Engg.,* **4** (3-4) : 140-142.

**Inderjeet, K. and Singh, S. M. (2008).** Seasonal arima model for forecasting of monthly rainfall and temperature. *Journal of Environmental Research & Development,* **3** : 2.

**Katz, R.W. and Skaggs, R.H. (1981).** On the use of autoregressive moving average processes to model meteorological time series, *Monthly Weather Rev.*, **109**: 479-484.

**Kumar, U., Meena, V.S., Singh, S., Bisht, J.K. and Pattanayak, A. (2021a).** Evaluation of digital elevation model in hilly region of Uttarakhand: FA case study of experimental farm

Hawalbagh. *Indian J. Soil Conserv.,* **49**: 77-81.

**Kumar, U., Panday, S.C., Kumar, J., Parihar, M., Meena, V.S., Bisht, J.K. and Kant, L. (2022).** Use of a decision support system to establish the best model for estimating reference evapotranspiration in subtemperate climate: Almora, Uttarakhand. *Agric. Eng. Int. CIGR J.,* **24** (1) : 41-50.

**Kumar, U., Singh D.K., Panday, S.C., Bisht, J.K and Kant, L. (2022).** Development and evaluation of seasonal rainfall forecasting (SARIMA) model for Kumaon region of Uttarakhand. *Indian Journal of Soil Conservation,* **50** (3) : 190-198.

**Kumar, U., Srivastava, A., Kumari, N., Rashmi, Sahoo, B., Chatterjee, C. and Raghuwanshi, N.S. (2021b).** Evaluation of spatio-temporal evapotranspiration using satellite-based approach and lysimeter in the agriculture dominated catchment. *J. Indian Soc. Remote Sens.,* **49** : 1939-1950.

**Mohan, S. and Arumugam, N., (1995).** Forecasting weekly reference evapotranspiration series. *Hydrological Science,* **40** (6) : 689-702.

**Nikam, Valmik B. and Meshram, B. B. (2013).** Modeling rainfall Prediction using data mining method: A Bayesian approach".Computational Intelligence, Modelling and Simulation (cimsim), 2013 Fifth International Conference on, 132-136,IEEE.

**Nury, A .H., Koch, M. and Alam, M.J.B. (2013).** Time series analysis and forecasting of temperatures in the sylhet division of Bangladesh, *Environmental Science*, 65-68pp.

**Popale, P. G. and Gorantiwar, S. D. (2014).** Stochastic generation and forecasting of weekly rainfall for Rahuri region *International Journal of Innovative Research in Science, Engineering & Technology,* **3** (4), April 2014 Two days National Conference – VISHWATECH 2014.

**Ram , B., Gaur , M. L., Patel , G. R., Kunapara , A. N. and& Damor, P.A. (2023a).** Stochastic disaggregation of daily rainfall using barlett lewis rectangular pulse model (BLRPM): A case study of middle Gujarat. *International Journal of Environment & Climate Change,* **13** (4) : 37–47. https://doi.org/10.9734/ijecc/2023/v13i41710.

**Ram, Bhavin, Gaur, Murari, Patel, Gautam, Kunapara, A., Pampaniya, Nirav, Damor, P. and Balas, Duda (2023b).** Assessment of diurnal variability and region-specific connection across intensity, Depth & Duration of Rainfall. *International Journal of Environment & Climate Change*, **13** : 595-606. 10.9734/ijecc/2023/v13i92275.

**Shivhare, N., Kumar, A.L., Dwivedi, S.B. and Dikshit, P.K.S. (2019).** ARIMA based daily weather forecasting tool: A case study for Varanasi. MAUSAM, **70** (1) : 133-140.

**Shoba, G. and Shobha, G. (2014).** Rainfall prediction using data mining techniques: A survey, *Int. J. Engg. & Computer Science,* **3** (5) : 6206-6211.